Discrete Time Crystal Enabled by Stark Many-Body Localization

Shuo Liu,[1,2] Shi-Xin Zhang,[2,*] Chang-Yu Hsieh,[2] Shengyu Zhang,[2] and Hong Yao[1,†]
[1]*Institute for Advanced Study, Tsinghua University, Beijing 100084, China*
[2]*Tencent Quantum Laboratory, Tencent, Shenzhen, Guangdong 518057, China*

(Received 15 August 2022; revised 11 November 2022; accepted 15 February 2023; published 23 March 2023)

Discrete time crystals (DTCs) have recently attracted increasing attention, but most DTC models and their properties are only revealed after disorder average. In this Letter, we propose a simple disorder-free periodically driven model that exhibits nontrivial DTC order stabilized by Stark many-body localization (MBL). We demonstrate the existence of the DTC phase by analytical analysis from perturbation theory and convincing numerical evidence from observable dynamics. The new DTC model paves a new promising way for further experiments and deepens our understanding of DTCs. Since the DTC order does not require special quantum state preparation and the strong disorder average, it can be naturally realized on the noisy intermediate-scale quantum hardware with much fewer resources and repetitions. Moreover, in addition to the robust subharmonic response, there are other novel robust beating oscillations in the Stark-MBL DTC phase that are absent in random or quasiperiodic MBL DTCs.

DOI: 10.1103/PhysRevLett.130.120403

Introduction.—Spontaneous symmetry breaking (SSB) is one of the most important concepts in modern physics. Various phases of matter and phase transitions can be described by the SSB mechanism; for example, the formation of crystals is the result of spontaneously breaking continuous spatial translational symmetry. Inspired by this notion, Wilczek proposed the intriguing concept of a "time crystal" that spontaneously breaks continuous time translational symmetry [1–3], and various no-go theorems [4–6] have established since then that the continuous time crystal would not exist. However, Floquet systems, quantum systems subject to periodic driving, can exhibit discrete time translational symmetry breaking [7–10] and have attracted considerable research interest [7,8,11–20]. The given observable in the discrete time crystal (DTC) phase can develop persistent oscillations whose period is an integer multiple of the driving period. Recently, DTCs have been experimentally realized in programmable quantum devices with periodic driving [21–26].

Because of the existence of periodic driving, energy is no longer conserved in a Floquet system. Thus, in the absence of any other local conservation laws, a generic system will absorb energy from the periodic driving, ultimately heating to infinite temperature. The thermalization of many-body Floquet systems implies that any local physical observable becomes featureless at late times [27–29]. Therefore, strong disorder is required [7–10,29–32] to realize many-body localization (MBL) that exhibits emergent local integrals of motion [33,34] and prevents absorption of heat from periodic driving. However, to investigate the DTC behavior, we have to average the observable dynamics over a great number of different disorder instances, requiring more quantum resources and severely restricting the efficient experimental study of DTCs.

Besides DTCs stabilized by the MBL phase, so-called a prethermal DTC phase exists without the need of MBL. Under some conditions, the dynamics of the many-body Floquet system can be thought of as being generated by an effective time-independent "prethermal Hamiltonian" $H_{\rm eff}$. The Floquet system can then display DTC dynamics upon starting from certain low-temperature symmetry-breaking initial states of $H_{\rm eff}$ within an exponential heating time window [35–39], realizing prethermal DTCs [11,40–45].

Recently, in the kicked PXP model [46,47], the discrete time crystal order enabled by quantum many-body scars [48–51] with the Néel state as the initial state has been identified, which is strongly reminiscent of a prethermal DTC. (See Ref. [52] for another similar mechanism enabling sub-Hilbert space DTC behavior in which the DTC lifetime can be enhanced with dynamical freezing [53–55].) The fidelity $F_n = |\langle Z_2|U_F^n|Z_2\rangle|^2$ is used to characterize the dynamics in this model, where $|Z_2\rangle$ is the initial Néel state and U_F is the Floquet evolution unitary. When n is even, $F_n > 0$ and when n is odd, $F_n = 0$; this corresponds to the subharmonic response with a timescale $T_s = 2$. After a long enough time, the fidelity will decay to zero finally and stay featureless, and this corresponds to the prethermal timescale T_p. Between the two timescales, there are another two novel timescales that have not been reported in DTC or prethermal DTC phases before. One is the emergent beating timescale T_b: the fidelity at even periods exhibits a beating oscillation that comes from the overlap between the Néel initial state and the lowest-lying excited states of $H_{\rm eff}$. The beating timescale $T_b \propto \Delta^{-1}$, where Δ is the gap in the Floquet spectrum. The other is the timescale T_g that is set by the inverse energy splitting in the ground state manifold and

$T_g \propto e^N$ where N is the system size. After driving cycles in the order of T_g, the fidelity at even periods F_{2n} decreases, while simultaneously the fidelity at odd periods F_{2n+1} increases. However, different from prethermal DTC phases, these phenomena strongly depend on special Néel initial states where highly accurate quantum state preparation is required.

An extremely important and exciting direction is to identify a clean Floquet system, i.e., without strong disorder, that exhibits a nontrivial DTC phase with no dependence on initial states. To stabilize this intrinsically dynamical phase, MBL is extremely important as discussed above. It has long been established that the quantum systems may enter MBL phases in the presence of sufficiently strong random disorder [33,34,56–64], quasiperiodic potential [65–70], or linear Zeeman field [71–75] in one-dimensional (1D) systems. The third one is called Stark MBL [71–76]. By intuition, we may construct a clean many-body Floquet system utilizing Stark MBL to stabilize DTC order.

In this Letter, we propose a clean kicked Floquet model inspired by Stark MBL. It has various nontrivial and interesting properties, including a robust subharmonic response as conventional DTC and other novel timescales similar to those reported in the kicked PXP model and Rydberg atom experiments [46,47]. The subharmonic response is robust against imperfection and does not depend on special initial states, which is a signal for a nontrivial DTC phase. Since the existence of DTC order does not depend on the strong disorder, it can be naturally realized on the quantum hardware, relying on fewer quantum computational resources and experimental trials.

Model.—The Floquet unitary for the model considered in the Letter reads as

$$U_F = U_2 U_1 = e^{-iH_2} e^{-i(\frac{\pi}{2}-\epsilon)H_1}, \tag{1}$$

where

$$H_1 = \sum_j X_j, \tag{2}$$

$$H_2 = J_z \sum_j (j+1) Z_j Z_{j+1} + W \sum_j j Z_j. \tag{3}$$

X and Z are Pauli matrices, and ϵ is the imperfection in the driving. H_1 is the kicked term, when $\epsilon = 0$, $U_1 = \prod_j X_j$ and all the spins flip exactly. H_2 has two terms: one is a linear Zeeman field for Stark MBL; the other one is a linear zz interaction. The linear term for interaction is important to stabilize a DTC similar to the case discussed in [23] (see also in the Supplemental Material [77]). The reason is that the linear Zeeman field, as well as the Stark MBL, will be suppressed by the imperfection ϵ. Therefore, we need some nonuniform interaction to stabilize the MBL phase. Different from the random MBL DTC case where a strong disorder in zz interaction is added, we here instead also use a linear zz interaction.

When $\epsilon = 0$, the quasieigenstates of U_F^0 can be written as

$$|\pm\rangle = \frac{1}{\sqrt{2}} \left(e^{-i\frac{H_2(z)}{2}} |z\rangle \pm e^{-i\frac{H_2(-z)}{2}} |-z\rangle \right), \tag{4}$$

whose eigenvalues are

$$U_F^0 |\pm\rangle = \pm e^{-i\frac{H_2(z)+H_2(-z)}{2}} |\pm\rangle, \tag{5}$$

respectively, where $|z\rangle$ is the product state and $|-z\rangle = \prod_j X_j |z\rangle$. $|+\rangle$ and $|-\rangle$ form a so-called π pair in which quasieigenenergy difference equals π. For simplicity, we use quasieigenenergy ε_F of $|+\rangle$ to represent this π pair. And for any product state $|z\rangle$, it can be represented by a superposition of a π pair of quasieigenstates,

$$|\pm z\rangle = \frac{1}{\sqrt{2}} e^{i\frac{H_2(\pm z)}{2}} (|+\rangle \pm |-\rangle). \tag{6}$$

Therefore, there is a trivial subharmonic response in $\epsilon = 0$ limit,

$$U_F^2 |z\rangle = U_F |-z\rangle = |z\rangle, \tag{7}$$

where we have ignored the global phase. Accordingly, the local physical observables, such as $\langle Z(t) \rangle$, develop persistent oscillations whose periods are twice the driving period, and the discrete time translational symmetry spontaneously breaks. However, this DTC order depends on fine-tuning of parameters $\epsilon = 0$. To establish a nontrivial DTC phase, the subharmonic response must be robust against imperfection ϵ. When $\epsilon \neq 0$, the quasieigenstates cannot be analytically exactly tracked; we use perturbation theory and numerical results below to show that the subharmonic response is robust against imperfection ϵ.

Observable.—To describe the dynamics of the kicked model and diagnose the DTC phase, we need to utilize suitable observables. Because of the linear Zeeman field and linear zz interaction, different spatial sites are not equivalent anymore. Therefore, we do not choose the nonequal time spin-spin correlation on site $N/2$ commonly used in previous DTC works [12] and instead use more representative site-averaged observables. Spurred by [47], we define two types of fidelity: One is the fidelity for a given initial state,

$$F_n = |\langle \psi_i | U_F^n | \psi_i \rangle|^2, \tag{8}$$

where $|\psi_i\rangle$ is the initial state. The other is the state-averaged fidelity

$$\bar{F}_n = \frac{1}{2^N} \sum_{\{z\}} |\langle z | U_F^n | z \rangle|^2, \tag{9}$$

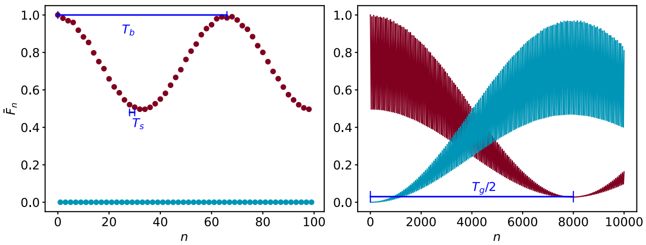

FIG. 1. Three timescales for the dynamics of the state-averaged fidelity $\bar{F}_n$: when n is even, $\bar{F}_n > 0$ and when n is odd, $\bar{F}_n = 0$, which correspond to the subharmonic response $T_s = 2$; in addition to this subharmonic response, there is a beating timescale $T_b \approx 66$ and a third timescale $T_g \approx 16\,000$ ($N = 3$; $J_z = (\pi/2N)$; $W = 5.0$; $\epsilon = 0.05$).

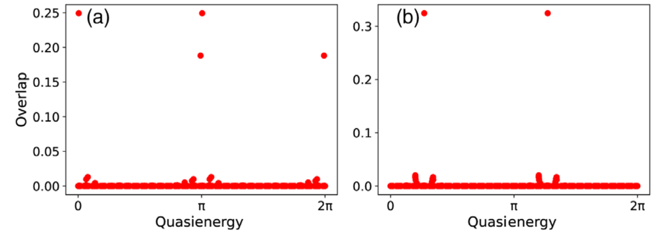

FIG. 2. Overlaps with quasieigenstates of U_F: $N = 15$; $J_z = (\pi/2N)$; $W = 5.0$; $\epsilon = 0.05$. (a) The product state $|000000000000000\rangle$ roughly lives in a subspace with dimension of four and we can see the obvious dominant-subleading π-pair pattern. (b) There is only one obvious π pair in the decomposition of the product state $|001100110011001\rangle$.

where the sum is over all possible 2^N product states $|z\rangle$. We can also utilize a site-averaged spin autocorrelator as the observable $\overline{\langle Z(0)Z(n)\rangle} = (1/N)\sum_j \langle Z_j(0)Z_j(nT)\rangle$, and the dynamical behaviors are qualitatively the same as the fidelity (see the Supplemental Material for details [77]).

Analysis of different timescales.—We observe three different timescales for our Floquet model, which are similar to those reported in the kicked PXP model. Because the third timescale $T_g \propto e^N$ is exponential with the system size, we show the dynamics of a small system (three sites) first to demonstrate all three timescales in the dynamics. The results are summarized in Fig. 1.

To understand these three timescales, we consider a product state $|z\rangle$ and the corresponding state-dependent fidelity first. When $\epsilon \neq 0$, although the product state $|z\rangle$ cannot be represented by a superposition of one π pair of quasieigenstates, we can still do decomposition in the eigenspace of U_F. Based on the perturbation theory, the quasieigenstate of U_F ($\epsilon \neq 0$) can be written as a superposition of the quasieigenstates of U_F^0 ($\epsilon = 0$) with the similar quasieigenenergies. For a given product state $|z\rangle$, the corresponding original π pair of quasieigenstates and the most related quasieigenstates to the first-order perturbation form a Hilbert subspace, and $|z\rangle$ roughly live in this subspace.

We utilize perturbation theory to locate the subspace where the product state $|z\rangle$ lives. We use $|\pm\rangle$ to represent the original π pair related to $|z\rangle$ when $\epsilon = 0$ and the quasieigenenergy is ε_F, i.e., $U_F^0|\pm\rangle = \pm e^{-i\varepsilon_F}|\pm\rangle$. By intuition, the dimension of the subspace is determined by the number of quasieigenstates of U_F^0 that have similar quasieigenenergies with $|\pm\rangle$. In the Supplemental Material [77], we show that if there is only one π pair of quasieigenstates $|\pm'\rangle$ with $\varepsilon'_F = \varepsilon_F$ or $\varepsilon_F + \pi (\mathrm{mod}\ 2\pi)$, $|\pm\rangle$ and $|\pm'\rangle$ form a subspace with dimension of four, and $|z\rangle$ roughly lives in this subspace. Equivalently, if we check the overlaps between $|z\rangle$ and quasieigenstates of U_F, there is an obvious dominant-subleading π-pair pattern, see Fig. 2(a). Even if there is no exactly matching quasieigenstates of U_F^0, as long as there is one special π pair of quasieigenstates of U_F^0 that has the closer quasieigenenergy with $|\pm\rangle$ than all other eigenstates, the dominant-subleading π-pair pattern for the decomposition of $|z\rangle$ still exists. On the contrary, if several π pairs of U_F^0 have the same closest quasieigenenergy difference with $|\pm\rangle$ as $\delta\varepsilon_F = |\varepsilon_F - \varepsilon'_F| = \delta$, the dominant-subleading π-pair pattern vanishes and we can only see one π pair (the original one) with dominant overlap, see Fig. 2(b).

When $\epsilon = 0$, the product state $|z\rangle$ can be represented by an equal weight superposition of a π pair of quasieigenstates of U_F^0 and this induces the subharmonic response as discussed above. When ϵ is small, as long as the product state $|z\rangle$ can still be represented by a superposition of several π pairs of quasieigenstates of U_F and the weights of the two quasieigenstates in any π pair have the same absolute value, as guaranteed by the perturbation theory, the $T_s = 2$ subharmonic response still exists.

The beating timescale T_b is caused by the quasieigenenergy difference between different quasieigenstates (see the Supplemental Material for details [77]). Consider a three-site subsystem of a product state $|z\rangle$, $|S_{j-1}, S_j, S_{j+1}\rangle$, $|z\rangle$ and $|-z\rangle(|-S_{j-1}, -S_j, -S_{j+1}\rangle)$ can be combined into a π pair with quasieigenenergy equal to $\{[H_2(z) + H_2(-z)]/2\}$ when $\epsilon = 0$. If we flip spin S_j of $|z\rangle$ and $|-z\rangle$, there are two new product states $|z'\rangle(|S_{j-1}, -S_j, S_{j+1}\rangle)$ and $|-z'\rangle(|-S_{j-1}, S_j, -S_{j+1}\rangle)$, and they form a new π pair $|\pm'\rangle$ with quasieigenenergy ε'_F. The quasieigenenergy difference between the two π pairs is

$$\delta\varepsilon_F = 2J_z|jS_{j-1} + (j+1)S_{j+1}| \pmod{2\pi}. \quad (10)$$

When $S_{j-1} = -S_{j+1}$, the quasieigenenergy difference after flipping the spin S_j equals $2J_z$; when $S_{j-1} = S_{j+1}$, the quasieigenenergy difference after flipping the spin S_j equals $2(2j+1)J_z$. Suppose $J_z = (\pi/2N)$ and assume N to be odd for simplicity; considering the spin configuration around a fixed site $[(N-1)/2]$ (the middle site), the product states can be divided into two parts: when $S_{[(N-1)/2]-1} = S_{[(N-1)/2]+1}$, as discussed above, there are

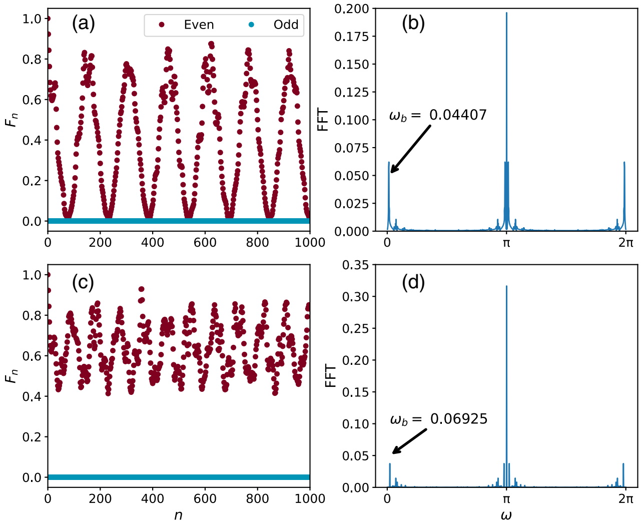

FIG. 3. Dynamics of the product state $|000000000000000\rangle$ which is a good initial state ($N = 15$; $W = 5.0$; $\epsilon = 0.05$). (a), (b) $J_z = (\pi/2N)$. (c),(d) $J_z = [(\pi - 0.05)/2N]$. In both cases, there is a dominant beating timescale.

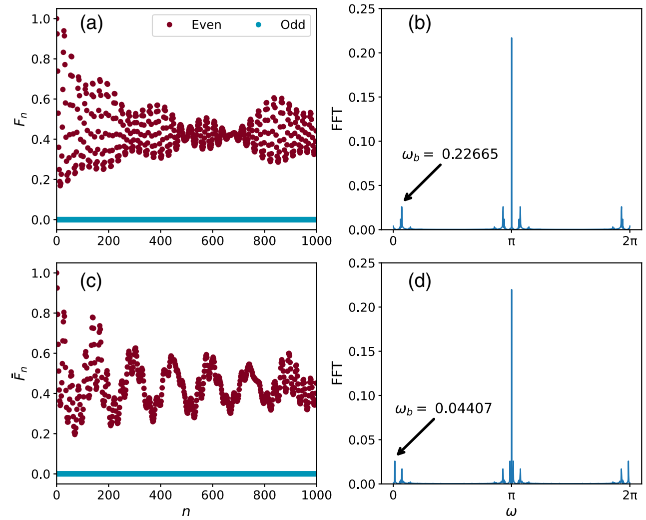

FIG. 4. (a),(b) Dynamics of the product state $|001100110011001\rangle$ ($N = 15$; $J_z = (\pi/2N)$; $W = 5.0$; $\epsilon = 0.05$). Such a bad initial state gives another beating timescale. (c),(d) Dynamics of the state-averaged fidelity $\bar{F}_n$ ($N = 15$; $J_z = (\pi/2N)$; $W = 5.0$; $\epsilon = 0.05$). The dominant beating timescale $T_b = (2\pi/\omega_b)$ is determined by the good initial states.

two π pairs related by a Pauli-X matrix at site $[(N-1)/2]$ and the quasieigenenergy difference is equal to π. Furthermore, the quasieigenstates decomposition of the product state includes a dominant π pair and a subleading π pair, see Fig. 2(a). We call these product states "good initial states." The dynamics of these good states have a dominant beating timescale T_b determined by the quasieigenenergy difference between dominant and subleading π pairs, and T_b fits well with the perturbative predictions (see the Supplemental Material for details [77]), see Fig. 3. When $S_{[(N-1)/2]-1} = -S_{[(N-1)/2]+1}$, there is no π pair $|\pm'\rangle$ with quasieigenenergy difference $\delta\varepsilon_F = 0$ or π with $|\pm\rangle$. As shown in Fig. 2(b), there is no dominant-subleading π-pair pattern. We call these product states "bad initial states." Although there is no obvious subleading π pair, there are still many π pairs with small overlaps and different quasieigenenergy differences with $|\pm\rangle$; thus we can see many Fourier peaks in Fig. 4(b) (see the Supplemental Material for details [77]).

Now we investigate the robustness of a beating timescale by considering nonperfect J_z, for example, $J_z = [(\pi - 0.05)/2N]$. For a π pair of quasieigenstates of U_F^0 combined by good initial states, although there is no other π pairs of quasieigenstates of U_F^0 with $\delta\varepsilon_F = 0$ or π, as long as only one π pair of quasieigenstates has closer quasieigenenergy with $|\pm\rangle$ than all other quasieigenstates, the dominant-subleading π-pair pattern still exists and there is a dominant beating timescale, see Fig. 3(d).

We can use a more general state-averaged observable, the state-averaged fidelity, to describe the dynamics of the many-body Floquet system. The quasieigenenergy corrections due to the first-order perturbation to all good initial states are the same, in the case considered here, $T_b \approx (\pi/\epsilon \sin\{[(N-1)/2]W\})$. Although there is another beating timescale for bad initial states, the dominant beating timescale for state-averaged quantities is determined by good initial states, see Fig. 4(d) (see the Supplemental Material for analytical analysis [77]). Additionally, there is no scaling relation between T_b and the system size N. Note that the classification of good and bad initial state is only for the beating timescale T_b; all initial states show a robust subharmonic response $T_s = 2$ breaking discrete time translational symmetry.

In terms of the timescale T_g, it is induced by the tiny quasienergy splitting of a given π pair, i.e., the quasieigenenergy difference between $|+\rangle$ and $|-\rangle$ equals $\pi + \delta$. This quasienergy mismatch δ due to the finite-size effect induces the third timescale as $T_g \propto (1/\delta)$ and $\delta \propto e^{-N}$ (see the Supplemental Material for details [77]). As discussed in [83], the existence of the third timescale T_g depends on the order of the two limits: (a) $\lim_{t\to\infty}\lim_{N\to\infty}$ and (b) $\lim_{N\to\infty}\lim_{t\to\infty}$, where (a) characterizes the "intrinsic" quench dynamics of this phase. In (a), we will never reach times of $O(e^N)$ and the third oscillation timescale T_g ($\propto e^N$) vanishes. We can only observe the subharmonic response and beating oscillation out to $t \to \infty$.

J_z with dependence on the system size N investigated in this Letter is designed to facilitate the analytical understanding of the beating timescale and is not necessary for the realization of a stable DTC phase. More numerical results with size-independent J_z can be found below and in the Supplemental Material [77].

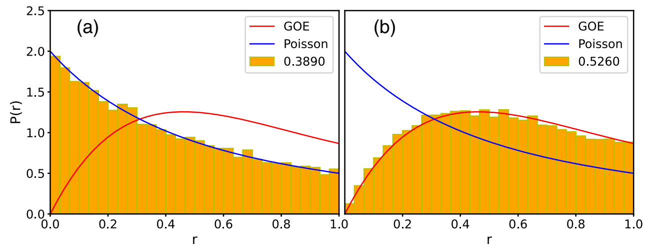

FIG. 5. Histogram of the distribution of the level spacing ratios: $N = 15$, $J_z = \pi + 1.5$, $W = 5.0$. (a) $\epsilon = 0.05$. (b) $\epsilon = 0.5$. With increasing the imperfection ϵ, the distribution of the level spacing ratio gradually crosses from the Poisson limit to the GOE distribution.

Phase transition.—In this section, we investigate the DTC order and choose the general size-independent J_z. To stabilize the DTC phase, MBL is extremely important as discussed above. As shown in Fig. 5, the distribution of the level spacing ratio [58] gradually crosses from the Poisson limit to the Gaussian orthogonal ensemble (GOE) with increasing imperfection ϵ, indicating a phase transition from MBL phase to trivial thermal phase.

To diagnose the phase transition and discrete time translational symmetry breaking, we utilize two indicators: the magnitude of the subharmonic response and the mutual information between the first and the last site. In principle, the critical imperfection ϵ_c can be extracted from the data collapses for mutual information [12]. Because of limitation of the system size accessible, the critical value ϵ_c and the critical exponents cannot be accurately determined for some Hamiltonian parameters (see more details on the finite-size data collapse in the Supplemental Material [77]). Nonetheless, the convincing numerical results indeed imply the existence of the DTC phase, see Fig. 6 for the schematic phase diagram. Even in the presence of a generic spin-spin interaction, the DTC phase still exists and is robust against the imperfection ϵ (see the Supplemental Material for more numerical results [77]).

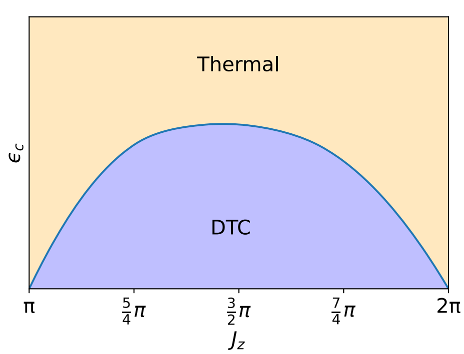

FIG. 6. The schematic phase diagram: when $J_z = n\pi$, the zz interaction has no effect on the Floquet evolution and the system enters the trivial thermalized phase.

Discussions and conclusion.—It was reported that Stark many-body localization can be induced by a strong external magnetic field even in the presence of a local phonon bath [76]. On the contrary, DTC stabilized by random disorder MBL is unstable against environmental coupling in open systems [84]. Because of the different mechanisms between random MBL and Stark MBL, an interesting future direction is to investigate whether the DTC phase enabled by Stark MBL is robust when coupling to the environment.

We have demonstrated that the discrete time crystal can be realized in a clean kicked Floquet model stabilized by Stark MBL. We also utilize the perturbation theory to explain the novel beating timescale absent in conventional DTC. Compared to the conventional DTC stabilized by the strong disorder, the resources required in our model are much fewer and it can be easily realized on the noisy intermediate-scale quantum hardware [85,86] (see the Supplemental Material for detailed experimental proposals [77]).

We thank Zhou-Quan Wan for helpful discussions. This work is supported in part by the MOSTC Grants No. 2021YFA1400100 and No. 2018YFA0305604 (H. Y.), the NSFC under Grant No. 11825404 (S. X. Z., S. L., and H. Y.), the CAS Strategic Priority Research Program under Grant No. XDB28000000 (H. Y.), and Beijing Municipal Science and Technology Commission under Grant No. Z181100004218001 (H. Y.).

[*]shixinzhang@tencent.com
[†]yaohong@tsinghua.edu.cn

[1] F. Wilczek, Quantum Time Crystals, Phys. Rev. Lett. **109**, 160401 (2012).
[2] T. Li, Z.-X. Gong, Z.-Q. Yin, H. T. Quan, X. Yin, P. Zhang, L.-M. Duan, and X. Zhang, Space-Time Crystals of Trapped Ions, Phys. Rev. Lett. **109**, 163001 (2012).
[3] F. Wilczek, Superfluidity and Space-Time Translation Symmetry Breaking, Phys. Rev. Lett. **111**, 250402 (2013).
[4] P. Bruno, Impossibility of Spontaneously Rotating Time Crystals: A No-Go Theorem, Phys. Rev. Lett. **111**, 070402 (2013).
[5] P. Nozières, Time crystals: Can diamagnetic currents drive a charge density wave into rotation?, Europhys. Lett. **103**, 57008 (2013).
[6] H. Watanabe and M. Oshikawa, Absence of Quantum Time Crystals, Phys. Rev. Lett. **114**, 251603 (2015).
[7] V. Khemani, A. Lazarides, R. Moessner, and S. L. Sondhi, Phase Structure of Driven Quantum Systems, Phys. Rev. Lett. **116**, 250401 (2016).
[8] D. V. Else, B. Bauer, and C. Nayak, Floquet Time Crystals, Phys. Rev. Lett. **117**, 090402 (2016).
[9] C. W. von Keyserlingk and S. L. Sondhi, Phase structure of one-dimensional interacting Floquet systems. II. Symmetry-broken phases, Phys. Rev. B **93**, 245146 (2016).
[10] C. W. von Keyserlingk, V. Khemani, and S. L. Sondhi, Absolute stability and spatiotemporal long-range order in Floquet systems, Phys. Rev. B **94**, 085112 (2016).

[11] K. Sacha, Modeling spontaneous breaking of time-translation symmetry, Phys. Rev. A **91**, 033617 (2015).
[12] N. Y. Yao, A. C. Potter, I.-D. Potirniche, and A. Vishwanath, Discrete Time Crystals: Rigidity, Criticality, and Realizations, Phys. Rev. Lett. **118**, 030401 (2017).
[13] A. Russomanno, F. Iemini, M. Dalmonte, and R. Fazio, Floquet time crystal in the Lipkin-Meshkov-Glick model, Phys. Rev. B **95**, 214307 (2017).
[14] Z. Gong, R. Hamazaki, and M. Ueda, Discrete Time-Crystalline Order in Cavity and Circuit QED Systems, Phys. Rev. Lett. **120**, 040404 (2018).
[15] B. Huang, Y.-H. Wu, and W. V. Liu, Clean Floquet Time Crystals: Models and Realizations in Cold Atoms, Phys. Rev. Lett. **120**, 110603 (2018).
[16] B. Zhu, J. Marino, N. Y. Yao, M. D. Lukin, and E. A. Demler, Dicke time crystals in driven-dissipative quantum many-body systems, New J. Phys. **21**, 073028 (2019).
[17] V. K. Kozin and O. Kyriienko, Quantum Time Crystals from Hamiltonians with Long-Range Interactions, Phys. Rev. Lett. **123**, 210602 (2019).
[18] K. Chinzei and T. N. Ikeda, Time Crystals Protected by Floquet Dynamical Symmetry in Hubbard Models, Phys. Rev. Lett. **125**, 060601 (2020).
[19] N. Y. Yao, C. Nayak, L. Balents, and M. P. Zaletel, Classical discrete time crystals, Nat. Phys. **16**, 438 (2020).
[20] H. P. Ojeda Collado, G. Usaj, C. A. Balseiro, D. H. Zanette, and J. Lorenzana, Emergent parametric resonances and time-crystal phases in driven Bardeen-Cooper-Schrieffer systems, Phys. Rev. Res. **3**, L042023 (2021).
[21] S. Choi, J. Choi, R. Landig, G. Kucsko, H. Zhou, J. Isoya, F. Jelezko, S. Onoda, H. Sumiya, V. Khemani, C. von Keyserlingk, N. Y. Yao, E. Demler, and M. D. Lukin, Observation of discrete time-crystalline order in a disordered dipolar many-body system, Nature (London) **543**, 221 (2017).
[22] J. Zhang, P. W. Hess, A. Kyprianidis, P. Becker, A. Lee, J. Smith, G. Pagano, I.-D. Potirniche, A. C. Potter, A. Vishwanath, N. Y. Yao, and C. Monroe, Observation of a discrete time crystal, Nature (London) **543**, 217 (2017).
[23] X. Mi *et al.*, Time-crystalline eigenstate order on a quantum processor, Nature (London) **601**, 531 (2021).
[24] J. Randall, C. E. Bradley, F. V. van der Gronden, A. Galicia, M. H. Abobeih, M. Markham, D. J. Twitchen, F. Machado, N. Y. Yao, and T. H. Taminiau, Many-body-localized discrete time crystal with a programmable spin-based quantum simulator, Science **374**, 1474 (2021).
[25] X. Zhang, W. Jiang, J. Deng, K. Wang, J. Chen, P. Zhang, W. Ren, H. Dong, S. Xu, Y. Gao, F. Jin, X. Zhu, Q. Guo, H. Li, C. Song, A. V. Gorshkov, T. Iadecola, F. Liu, Z.-X. Gong, Z. Wang, D.-L. Deng, and H. Wang, Digital quantum simulation of Floquet symmetry-protected topological phases, Nature (London) **607**, 468 (2022).
[26] P. Frey and S. Rachel, Realization of a discrete time crystal on 57 qubits of a quantum computer, Sci. Adv. **8**, eabm7652 (2022).
[27] L. D'Alessio and M. Rigol, Long-Time Behavior of Isolated Periodically Driven Interacting Lattice Systems, Phys. Rev. X **4**, 041048 (2014).
[28] A. Lazarides, A. Das, and R. Moessner, Equilibrium states of generic quantum systems subject to periodic driving, Phys. Rev. E **90**, 012110 (2014).
[29] P. Ponte, A. Chandran, Z. Papić, and D. A. Abanin, Periodically driven ergodic and many-body localized quantum systems, Ann. Phys. (Amsterdam) **353**, 196 (2015).
[30] P. Ponte, Z. Papić, F. Huveneers, and D. A. Abanin, Many-Body Localization in Periodically Driven Systems, Phys. Rev. Lett. **114**, 140401 (2015).
[31] A. Lazarides, A. Das, and R. Moessner, Fate of Many-Body Localization under Periodic Driving, Phys. Rev. Lett. **115**, 030402 (2015).
[32] D. A. Abanin, W. D. Roeck, and F. Huveneers, Theory of many-body localization in periodically driven systems, Ann. Phys. (Amsterdam) **372**, 1 (2016).
[33] M. Serbyn, Z. Papić, and D. A. Abanin, Local Conservation Laws and the Structure of the Many-Body Localized States, Phys. Rev. Lett. **111**, 127201 (2013).
[34] D. A. Huse, R. Nandkishore, and V. Oganesyan, Phenomenology of fully many-body-localized systems, Phys. Rev. B **90**, 174202 (2014).
[35] D. A. Abanin, W. De Roeck, and F. Huveneers, Exponentially Slow Heating in Periodically Driven Many-Body Systems, Phys. Rev. Lett. **115**, 256803 (2015).
[36] T. Mori, T. Kuwahara, and K. Saito, Rigorous Bound on Energy Absorption and Generic Relaxation in Periodically Driven Quantum Systems, Phys. Rev. Lett. **116**, 120401 (2016).
[37] T. Kuwahara, T. Mori, and K. Saito, Floquet-magnus theory and generic transient dynamics in periodically driven many-body quantum systems, Ann. Phys. (Amsterdam) **367**, 96 (2016).
[38] D. A. Abanin, W. De Roeck, W. W. Ho, and F. Huveneers, Effective Hamiltonians, prethermalization, and slow energy absorption in periodically driven many-body systems, Phys. Rev. B **95**, 014112 (2017).
[39] D. Abanin, W. De Roeck, W. W. Ho, and F. Huveneers, A rigorous theory of many-body prethermalization for periodically driven and closed quantum systems, Commun. Math. Phys. **354**, 809 (2017).
[40] D. V. Else, B. Bauer, and C. Nayak, Prethermal Phases of Matter Protected by Time-Translation Symmetry, Phys. Rev. X **7**, 011026 (2017).
[41] T.-S. Zeng and D. N. Sheng, Prethermal time crystals in a one-dimensional periodically driven Floquet system, Phys. Rev. B **96**, 094202 (2017).
[42] D. J. Luitz, R. Moessner, S. L. Sondhi, and V. Khemani, Prethermalization Without Temperature, Phys. Rev. X **10**, 021046 (2020).
[43] A. Kyprianidis, F. Machado, W. Morong, P. Becker, K. S. Collins, D. V. Else, L. Feng, P. W. Hess, C. Nayak, G. Pagano, N. Y. Yao, and C. Monroe, Observation of a prethermal discrete time crystal, Science **372**, 1192 (2021).
[44] M. Natsheh, A. Gambassi, and A. Mitra, Critical properties of the prethermal Floquet time crystal, Phys. Rev. B **103**, 224311 (2021).
[45] W. C. Yu, J. Tangpanitanon, A. W. Glaetzle, D. Jaksch, and D. G. Angelakis, Discrete time crystal in globally driven interacting quantum systems without disorder, Phys. Rev. A **99**, 033618 (2019).

[46] D. Bluvstein, A. Omran, H. Levine, A. Keesling, G. Semeghini, S. Ebadi, T. T. Wang, A. A. Michailidis, N. Maskara, W. W. Ho, S. Choi, M. Serbyn, M. Greiner, V. Vuletić, and M. D. Lukin, Controlling quantum many-body dynamics in driven Rydberg atom arrays, Science **371**, 1355 (2021).
[47] N. Maskara, A. A. Michailidis, W. W. Ho, D. Bluvstein, S. Choi, M. D. Lukin, and M. Serbyn, Discrete Time-Crystalline Order Enabled by Quantum Many-Body Scars: Entanglement Steering via Periodic Driving, Phys. Rev. Lett. **127**, 090602 (2021).
[48] C. J. Turner, A. A. Michailidis, D. A. Abanin, M. Serbyn, and Z. Papić, Weak ergodicity breaking from quantum many-body scars, Nat. Phys. **14**, 745 (2018).
[49] W. W. Ho, S. Choi, H. Pichler, and M. D. Lukin, Periodic Orbits, Entanglement, and Quantum Many-Body Scars in Constrained Models: Matrix Product State Approach, Phys. Rev. Lett. **122**, 040603 (2019).
[50] M. Schecter and T. Iadecola, Weak Ergodicity Breaking and Quantum Many-Body Scars in Spin-1 *xy* Magnets, Phys. Rev. Lett. **123**, 147201 (2019).
[51] M. Serbyn, D. A. Abanin, and Z. Papić, Quantum many-body scars and weak breaking of ergodicity, Nat. Phys. **17**, 675 (2021).
[52] M. Collura, A. De Luca, D. Rossini, and A. Lerose, Discrete Time-Crystalline Response Stabilized by Domain-Wall Confinement, Phys. Rev. X **12**, 031037 (2022).
[53] A. Haldar, R. Moessner, and A. Das, Onset of Floquet thermalization, Phys. Rev. B **97**, 245122 (2018).
[54] A. Haldar, D. Sen, R. Moessner, and A. Das, Dynamical Freezing and Scar Points in Strongly Driven Floquet Matter: Resonance vs Emergent Conservation Laws, Phys. Rev. X **11**, 021008 (2021).
[55] A. Haldar and A. Das, Statistical mechanics of Floquet quantum matter: Exact and emergent conservation laws, J. Phys. Condens. Matter **34**, 234001 (2022).
[56] I. V. Gornyi, A. D. Mirlin, and D. G. Polyakov, Interacting Electrons in Disordered Wires: Anderson Localization and Low-t Transport, Phys. Rev. Lett. **95**, 206603 (2005).
[57] D. M. Basko, I. L. Aleiner, and B. L. Altshuler, Metal–insulator transition in a weakly interacting many-electron system with localized single-particle states, Ann. Phys. (Amsterdam) **321**, 1126 (2006).
[58] V. Oganesyan and D. A. Huse, Localization of interacting fermions at high temperature, Phys. Rev. B **75**, 155111 (2007).
[59] M. Znidaric, T. Prosen, and P. Prelovsek, Many-body localization in the Heisenberg *xxz* magnet in a random field, Phys. Rev. B **77**, 064426 (2008).
[60] C. Monthus and T. Garel, Many-body localization transition in a lattice model of interacting fermions: Statistics of renormalized hoppings in configuration space, Phys. Rev. B **81**, 134202 (2010).
[61] E. Cuevas, M. Feigel'man, L. Ioffe, and M. Mezard, Level statistics of disordered spin-1/2 systems and materials with localized Cooper pairs, Nat. Commun. **3**, 1128 (2012).
[62] J. H. Bardarson, F. Pollmann, and J. E. Moore, Unbounded Growth of Entanglement in Models of Many-Body Localization, Phys. Rev. Lett. **109**, 017202 (2012).
[63] R. Vosk and E. Altman, Many-Body Localization in One Dimension as a Dynamical Renormalization Group Fixed Point, Phys. Rev. Lett. **110**, 067204 (2013).
[64] M. Serbyn, Z. Papić, and D. A. Abanin, Universal Slow Growth of Entanglement in Interacting Strongly Disordered Systems, Phys. Rev. Lett. **110**, 260601 (2013).
[65] S. Iyer, V. Oganesyan, G. Refael, and D. A. Huse, Many-body localization in a quasiperiodic system, Phys. Rev. B **87**, 134202 (2013).
[66] R. Modak and S. Mukerjee, Many-Body Localization in the Presence of a Single-Particle Mobility Edge, Phys. Rev. Lett. **115**, 230401 (2015).
[67] S.-X. Zhang and H. Yao, Universal Properties of Many-Body Localization Transitions in Quasiperiodic Systems, Phys. Rev. Lett. **121**, 206601 (2018).
[68] T. Kohlert, S. Scherg, X. Li, H. P. Lüschen, S. Das Sarma, I. Bloch, and M. Aidelsburger, Observation of Many-Body Localization in a One-Dimensional System with a Single-Particle Mobility Edge, Phys. Rev. Lett. **122**, 170403 (2019).
[69] S.-X. Zhang and H. Yao, Strong and weak many-body localizations, arXiv:1906.00971.
[70] S. Ghosh, J. Gidugu, and S. Mukerjee, Transport in the nonergodic extended phase of interacting quasiperiodic systems, Phys. Rev. B **102**, 224203 (2020).
[71] M. Schulz, C. A. Hooley, R. Moessner, and F. Pollmann, Stark Many-Body Localization, Phys. Rev. Lett. **122**, 040606 (2019).
[72] E. V. H. Doggen, I. V. Gornyi, and D. G. Polyakov, Stark many-body localization: Evidence for Hilbert-space shattering, Phys. Rev. B **103**, L100202 (2021).
[73] E. P. L. van Nieuwenburg, Y. Baum, and G. Refael, From Bloch oscillations to many body localization in clean interacting systems, Proc. Natl. Acad. Sci. U.S.A. **116**, 9269 (2019).
[74] V. Khemani, M. Hermele, and R. M. Nandkishore, Localization from Hilbert space shattering: From theory to physical realizations, Phys. Rev. B **101**, 174204 (2020).
[75] D. S. Bhakuni and A. Sharma, Entanglement and thermodynamic entropy in a clean many-body-localized system, J. Phys. Condens. Matter **32**, 255603 (2020).
[76] S. Sarkar and B. Buca, Protecting coherence from environment via Stark many-body localization in a quantum-dot simulator, arXiv:2204.13354.
[77] See Supplemental Material at http://link.aps.org/supplemental/10.1103/PhysRevLett.130.120403 for details, including the following: (1) the perturbation theory for dominant-subleading π-pair pattern, (2) analysis of different timescales, (3) the Fourier transform on the fidelity dynamics, (4) the numerical results for different imperfection ϵ, (5) level statistics for many-body localization, (6) the numerical results with different choices of J_z and W, (7) the dynamics of the autocorrelator, (8) phase transition and the impact of the generic interaction, and (9) the realization of DTC on quantum computers, which includes Refs. [78–82].
[78] R. Santagati, J. Wang, A. A. Gentile, S. Paesani, N. Wiebe, J. R. McClean, S. Morley-Short, P. J. Shadbolt, D. Bonneau, J. W. Silverstone, D. P. Tew, X. Zhou, J. L. O'Brien, and

M. G. Thompson, Witnessing eigenstates for quantum simulation of Hamiltonian spectra, Sci. Adv. **4** (2018).

[79] S. Liu, S.-X. Zhang, C.-Y. Hsieh, S. Zhang, and H. Yao, Probing many-body localization by excited-state variational quantum eigensolver, Phys. Rev. B **107**, 024204 (2023).

[80] Y. Y. Atas, E. Bogomolny, O. Giraud, and G. Roux, Distribution of the Ratio of Consecutive Level Spacings in Random Matrix Ensembles, Phys. Rev. Lett. **110**, 084101 (2013).

[81] M. M. Wolf, F. Verstraete, M. B. Hastings, and J. I. Cirac, Area Laws in Quantum Systems: Mutual Information and Correlations, Phys. Rev. Lett. **100**, 070502 (2008).

[82] C.-M. Jian, I. H. Kim, and X.-L. Qi, Long-range mutual information and topological uncertainty principle, arXiv:1508.07006.

[83] V. Khemani, R. Moessner, and S. L. Sondhi, A brief history of time crystals, arXiv:1910.10745.

[84] A. Lazarides and R. Moessner, Fate of a discrete time crystal in an open system, Phys. Rev. B **95**, 195135 (2017).

[85] J. Preskill, Quantum computing in the NISQ era and beyond, Quantum **2**, 79 (2018).

[86] F. Arute *et al.*, Quantum supremacy using a programmable superconducting processor, Nature (London) **574**, 505 (2019).